Neutron-Helium Interaction. II. Angular Distributions and Phase Shifts from 0.2 to 7.0 MeV*

G. L. MORGAN† AND R. L. WALTER
Duke University, Durham, North Carolina

(Received 31 August 1967; revised manuscript received 2 January 1968)

Precision relative differential cross sections for the scattering of neutrons from helium were measured at 22 neutron energies between 0.2 and 7.0 MeV. The measurements were made by observing the energy distribution of the recoiling helium nuclei in a high-pressure helium-gas scintillation counter irradiated by monoenergetic neutrons. An analysis of the data was made in terms of phase shifts. The data could be satisfactorily represented without the use of partial waves higher than $l=1$. The energy dependence of the phase shifts was found to be in good agreement with that predicted by single-level dispersion theory. Proton-helium phase shifts were calculated from the neutron-helium phase shifts and found to be in fair agreement with the existing data. It is shown that a Saxon-Woods potential can accurately represent the scattering of protons and neutrons from helium for energies at least up to 5 and 8 MeV, respectively.

I. INTRODUCTION

IN the preceding paper,[1] an attempt to extract scattering phase shifts for the neutron-helium interaction from polarization data obtained at two energies has been reported. The data were found to be somewhat inconsistent with the existing sets of phase shifts and indicated a need for further study of the n-He problem at low energies. Since data at a large number of energies was required to obtain a continuous set of phase shifts, cross-section data, although not necessarily as sensitive as polarization data, was taken, since it could be accumulated more rapidly. However, it was recognized that in order to be of any use the measurements had to have a high degree of accuracy. A brief review of the earlier, pertinent reports follows.

Until recently, the most trusted set of phase shifts for the energy region below 10 MeV were the set (DGS) proposed in 1952 by Dodder and Gammel.[2] These phase shifts were derived from the then existing proton-helium phase shifts using single-level dispersion theory and assuming the charge independence of nuclear forces. There have been a number of measurements of the neutron-helium scattering cross sections which were intended to test these phase shifts. (Reviews of this work prior to 1962 have been given by Hodgson[3] and Austin *et al.*[4]) There were basically two approaches. One was to measure cross sections and compare them to cross sections calculated from the phase shifts. These measurements generally confirmed the DGS phase shifts to within their experimental uncertainty. The other approach was to derive phase shifts from the data and to compare these with the DGS values. In general, these measurements produced phase shifts which showed some disagreement with the DGS values, particularly in the energy region around 1 to 4 MeV, where the experimental values of the $P_{1/2}$ phase shifts were often 5° to 10° below those of DGS. The situation was left in an unsettled condition, which is perhaps what one would expect if the cross section was not very sensitive to the phase shifts.

Several measurements have been performed since those of Austin *et al.* In 1963 Young *et al.*[5] measured an angular distribution at 1.79 MeV and concluded that their data was in agreement with cross sections calculated from the DGS phase shifts. However, their data was not considered to be accurate enough to be conclusive. In the same year May, Walter, and Barschall[6] made measurements of the angular dependence of the asymmetry in the scattering of polarized neutrons. As was mentioned in the preceding paper, they found agreement within the accuracy of their measurements with the DGS phase shifts below 10 MeV.

A general survey of the situation was made in 1966 by Hoop and Barschall,[7] who also reported angular distributions from 6 to 30 MeV, with particular emphasis on the $D_{3/2}$ state at an excitation energy of 16.7 MeV. They present a set of phase shifts (HB) which are based on two independent sets of previously determined phase shifts. Below 10 MeV they concluded that the DGS phase shifts (with the $P_{3/2}$ phase shift modified slightly to give better agreement with the total cross-section data) gave a satisfactory representation of the existing data. Above 14 MeV they showed that phase shifts calculated from proton-helium phase shifts (derived by Weitkamp and Haeberli[8] from polarization data) were in agreement with their data. The two sets of phase shifts were joined in a smooth way from 10 to 17 MeV. Their analysis showed that below 6 MeV the existing data could be satisfactorily repre-

* Work supported in part by the U. S. Atomic Energy Commission.

† NASA Graduate Fellow. Present address: University of Basel, Basel, Switzerland.

[1] J. R. Sawers, Jr., G. L. Morgan, L. A. Schaller, and R. L. Walter, preceding paper, Phys. Rev. **168**, 1102 (1968).

[2] D. C. Dodder and J. L. Gammel, Phys. Rev. **88**, 520 (1952).

[3] P. E. Hodgson, Phil. Mag. Suppl. **7**, 1 (1958).

[4] S. M. Austin, H. H. Barschall, and R. E. Shamu, Phys. Rev. **126**, 1532 (1962).

[5] P. G. Young, G. G. Ohlsen, and P. L. Okhuysen, Australian J. Phys. **16**, 185 (1963).

[6] T. H. May, R. L. Walter, and H. H. Barschall, Nucl. Phys. **45**, 17 (1963).

[7] B. Hoop and H. H. Barschall, Nucl. Phys. **83**, 65 (1966).

[8] W. G. Weitkamp and W. Haeberli, Nucl. Phys. **83**, 46 (1966).

sented without the use of d waves. It was also found that the s-wave phase shift could be represented by a hard-sphere phase shift with a hard-sphere radius of 2.4 F.

Sawers *et al.* in the preceding paper[1] derived phase shifts at 1.01 and 2.44 MeV from their polarization data. Their values disagreed somewhat with the sets proposed by DGS and HB.

In the experiment described here, relative differential cross sections for the scattering of neutrons from helium were obtained at 22 neutron energies between 0.2 and 7.0 MeV. The measurements were made by observing the energy distribution of the recoiling helium nuclei in a high-pressure helium gas scintillation counter irradiated by monoenergetic neutrons. The $Li^7(p,n)Be^7$, $C^{12}(d,n)N^{13}$, $T(p,n)He^3$, and $D(d,n)He^3$ reactions were used as neutron sources. Pulsed beam techniques were employed in conjunction with two-dimensional pulse-height analysis by an on-line computer in order to acquire detailed information on the correlation between time-of-flight and scintillation pulse height for the radiation incident on the counter. This procedure allowed discrimination against events in the counter produced by γ rays and energy-degraded neutrons.

Prior to the cross-section measurement, studies were conducted on the energy resolution and energy-to-pulse-height characteristics of the helium scintillation counter. The results of these studies were used to correct the measured helium recoil distributions for instrumental effects. Additional corrections were made for multiple scattering on the basis of distributions calculated by a random-walk procedure.

An analysis of the data was made in terms of phase shifts. A major problem encountered in the analysis was the lack of accurate total cross-section data required to convert the relative distributions to absolute differential cross sections. Previous investigations[3,4,7] had shown the s-wave phase shift to be well represented by a hard-sphere phase shift. Using this fact an alternate normalization procedure was chosen whereby the distributions at each energy were normalized such that they were consistent with an s-wave phase shift given by the hard-sphere value for that energy.

II. EXPERIMENTAL APPARATUS

A. Helium Gas Scintillation Counter

The helium gas scintillation counter used in the present measurement is shown in Fig. 1. It was constructed of brass and had walls which were 0.14 cm thick in the area subject to irradiation. The inner walls of the cell were coated with an aluminum film over which was applied a layer of magnesium oxide. An organic wavelength shifter was then evaporated over the magnesium oxide as well as on the inner surface of the plate glass window used to seal the viewing end of the cell. The counter was filled with a mixture of 65 atm of helium and 4.5 atm of xenon. An RCA 6810-A photomultiplier tube, placed in firm contact with the plate glass window, was used to measure the light produced by the scintillation in the gas.

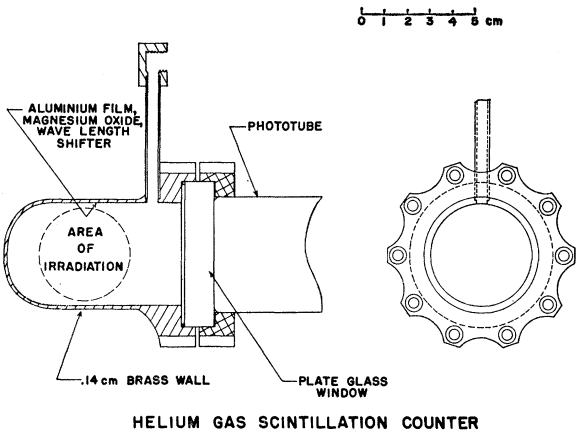

FIG. 1. Cross-sectional view of the helium gas scintillation counter.

There are several properties of the scintillation counter which had to be determined in order to correct the helium recoil distributions for instrumental effects. These properties include (1) the linearity of the energy-to-pulse-height conversion process, (2) the shape of the energy resolution function (defined as the pulse-height distribution resulting from monoenergetic events occurring over the active volume of the counter), and (3) the energy dependence of the resolution (defined here as the full width at half-maximum divided by the average pulse height for the pulse-height distribution described above). A detailed investigation of these properties was made in conjunction with the present work and has been reported elsewhere.[9] A brief summary of the

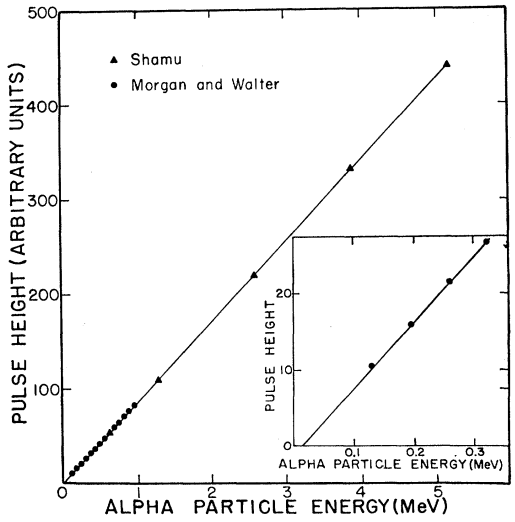

FIG. 2. Results of the linearity measurements for helium scintillations. The inset shows an expanded view of the very-low-energy data and indicates the nonzero intercept. This incorporates the data of Morgan and Walter and Shamu, as given in Ref. 9.

[9] G. L. Morgan and R. L. Walter, Nucl. Instr. Methods **58**, 277, (1968). See also R. E. Shamu, *ibid.* **14**, 297 (1962).

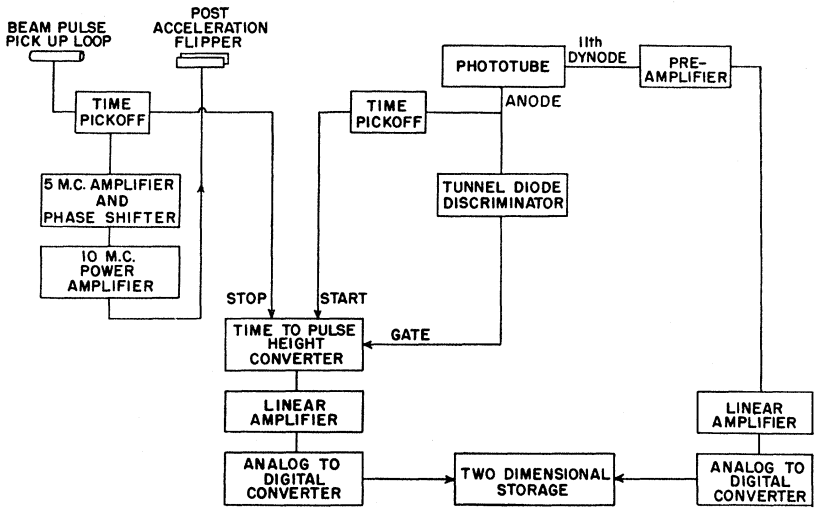

FIG. 3. Block diagram of the electronics used in the experiment.

points significant to the present analysis will be given here.

The energy-to-pulse-height properties of the helium scintillation counter are illustrated in Fig. 2. For recoil energies above 0.3 MeV the pulse-height-to-energy relation is linear, but not proportional. A straight line through the high-energy data extrapolates through 14 keV at zero pulse height. The data below 0.3 MeV indicates a tendency to curve through zero energy at zero pulse height. The data at all energies could be well represented by a linear form with the addition of a small exponential term. This relation was used to assign a recoil energy to a given pulse height, and to correct the pulse-height distributions for differential nonlinearity.

The energy variation of the magnitude of the energy resolution was found[9] to be in good agreement with what would be expected from the combination of an energy-independent contribution due to variation in light collection efficiency for different regions of the counter and of an energy-dependent contribution due to the statistical fluctuation in the number of photons, photoelectrons, and secondary electrons produced in the scintillation and detection process. Thus the energy dependence of the resolution can be expressed as

$$R^2 = R_v^2 + R_E^2, \qquad R_E \propto E^{-1/2}, \qquad (1)$$

where R is the over-all resolution of the counter, R_v is the resolution due to variation in light collection efficiency, and R_E is the resolution due to statistical fluctuations. The study indicated that R_v was about 0.08.

It was determined that the resolution function was very nearly Gaussian in shape. There were small deviations from a Gaussian shape for high-energy events (α-particle energies greater than 3 MeV), where the statistical contribution was small ($R_E \sim 0.05$); that is, where the resolution was mainly that due to variation in light collection efficiency. The effect of this non-Gaussian shape on the recoil spectrum was investigated in detail and the results are discussed later.

B. Accelerator and Beam Pulsing System

Monoenergetic neutrons were produced by nuclear reactions initiated by ion beams from the Duke University 4-MV Van de Graaff accelerator. The size of the ion beam was defined by means of a collimator located 15 cm from the target. The beam pulsing system is described in detail by Lewis *et al.*[10] The beam was initially pulsed in the terminal of the accelerator. The resulting pulses were about 10 nsec in duration with a 5-MHz repetition rate. After momentum analysis by a 60° deflection magnet, the pulses passed through a sensing element (pickup loop) in the beam tube. A block diagram of the associated electronics is shown in Fig. 3. A signal from the pickup loop controlled the phase of a 5-MHz amplifier which in turn drove a 10-MHz power amplifier. The output of the power amplifier was applied across a set of deflection plates located in the beam tube 0.5 m behind the pickup loop and 2 m in front of a beam defining slit. The resulting beam bursts at the target were about 5 nsec in duration. The target area was shielded by a concrete wall from possible background neutrons originating at the defining slit.

The neutron beam resulting from the source reaction was collimated to subtend a half-angle of 1° with respect to the source. This produced a neutron beam 4 cm in diameter at the helium cell which was located 1 m from the target. The area of the counter which was irradiated is shown in Fig. 1. In a manner consistent with reasonable counting rates, this collimation minimized the amount of counter wall which was exposed to the neutron beam. It also kept to a minimum that region of the counter in which recoil events could occur near the cell wall.

[10] H. W. Lewis, P. R. Bevington, W. W. Roland, R. L. Rummel, and R. W. Wilenzick, Rev. Sci. Instr. **30**, 923 (1959).

C. Electronics

A block diagram of the electronics associated with the scintillator is also shown in Fig. 3. The signal from the pickup loop served as a time marker for the time-to-pulse-height converter. The other marker was supplied by a time pickoff circuit which was triggered by fast pulses from the anode of the helium photomultiplier. This fast signal was also used as the input to a fast discriminator which supplied a gate to the time-to-pulse-height converter. Simultaneously with the timing signal, a slow signal, proportional to the light output of the scintillator, was taken from the 11th dynode of the photomultiplier. This linear signal was amplified by a linear amplifier having a 1-μsec clipping line. The linear and time-of-flight signals were fed into analog-to-digital converters (ADC), whose outputs were tied into an on-line computer[11] for two-dimensional analysis.

The linearity of electronics processing the "linear signal" was checked periodically and was determined to be linear to within 0.1%. However, the pulse height for zero channel number in the ADC was found to be 0.005 of the full-scale pulse-height value. The pulse-height distributions were corrected for this effect.

Cuts along the time-of-flight axis for a typical two-dimensional spectrum are shown in Fig. 4. Each of the spectra shown is the time-of-flight spectrum for a helium scintillator pulse height corresponding to a given c.m. scattering angle for the primary neutron group. The $Li^7(p,n)Be^7$ reaction was the neutron source, the energy of the primary neutron group being 1.3 MeV. Indicated by the labels are the neutron groups leaving Be^7 in its ground state and its first excited state (at 432 keV) and the prompt γ ray. In addition, there is a time-uncorrelated background which consists of photomultiplier noise and of neutrons and γ rays which have scattered in the room before entering the counter. The spectra for the other source reactions were similar to this one, but the $Li^7(p,n)Be^7$ reaction was the only one which produced two neutron groups.

In each time-of-flight spectrum, those channels which contained the primary neutron group were summed to provide one point in the one-dimensional helium recoil spectrum. In each case a correction was made for the time-uncorrelated background on the basis of the flat portion of that particular time-of-flight spectrum. These time-uncorrelated background corrections were less than 5% for all usable helium recoil channels at neutron energies above 1 MeV. For the lowest channels at lowest neutron energies (where the forward angle cross sections are small) this correction was as large as 25%.

[11] N. R. Roberson, D. R. Tilley, and M. B. Lewis, Bull. Am. Phys. Soc. **10**, 55 (1965). The computer used in the present work was model DDP-224, manufactured by Computer Control Company, Framingham, Mass.

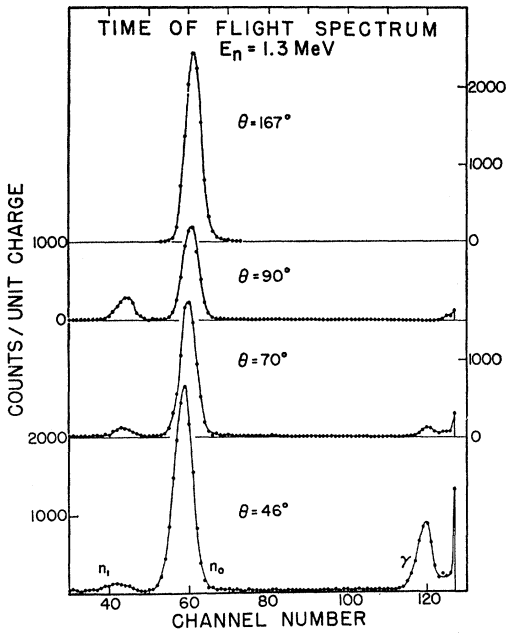

FIG. 4. Several time-of-flight spectra for a typical two-dimensional pulse-height spectrum. The $Li^7(p,n)Be^7$ reaction was the neutron source.

III. DATA ACCUMULATION

A. General

The measurement of an angular distribution at a given energy consisted of the accumulation of a two-dimensional spectrum (time-of-flight versus scintillation pulse-height) plus any necessary background measurements. Data-taking runs were limited to about 1 h in order to minimize the effects of drift in the electronics. If one such run was not sufficient to provide good counting statistics then the run was repeated as often as necessary. Each of these separate runs was checked against the others for possible drift and if none was found they were added together to form one spectrum. In all cases above 0.5 MeV neutron energy there are at least 3000 counts per channel in the one-dimensional helium recoil spectrum, with about 70 channels per spectrum.

The energy of the neutrons was calculated on the basis of the accelerator voltage, which was measured by means of a generating voltmeter.[12] This device was calibrated frequently using the threshold of the $Li^7(p,n)Be^7$ reaction. The uncertainty in the determination of the average neutron energy was 10 keV or less at all energies.

B. Data Acquisition

For neutron energies in the range from 0.2 to 1.3 MeV the $Li^7(p,n)Be^7$ reaction was used as a neutron source. The targets consisted of lithium metal evapo-

[12] C. E. Hollandsworth, S. G. Buccino, and P. R. Bevington, Nucl. Instr. Methods **28**, 353 (1964).

rated onto a tantalum backing. The spread in neutron energies produced by these targets was about 10 keV at neutron energies below 0.5 MeV and varied smoothly from 18 to 10 keV for neutron energies from 0.5 to 1.3 MeV, respectively. The neutron-production and helium cross sections were sufficiently large that each energy point could be completed in approximately 1 h.

For neutron energies of 1.96, 2.45, and 2.98 MeV, the $C^{12}(d,n)N^{13}$ reaction was employed. The targets were self-supporting carbon foils mounted on a holder of small mass located 5 cm in front of a beam catcher. A reaction angle of 30° was used in order to take advantage of the maximum in the cross section here and to allow the neutron collimator to shield the helium cell from the beam catcher. For the lower two energies, foils of about 40 keV in thickness were used, while at the higher energy an 80-keV foil was used. At each energy three runs were required to obtain good counting statistics. In addition, an extra run with the foil removed was made as a check on background neutron sources. These were negligible.

Data was also taken for neutron energies of 1.7 and 2.2 MeV using the $T(p,n)He^3$ reaction. The $C^{12}(d,n)N^{13}$ reaction is not a commonly used neutron source (the prompt γ ray is quite intense) so checks were made in this energy range using a more standard neutron source reaction. The target consisted of tritium absorbed in a layer of erbium which had been evaporated onto a copper backing. The neutron energy spread from this target was approximately 30 keV. Three data runs were required to accumulate a sufficient number of events.

Neutrons of 5 to 7 MeV in energy were obtained from the $D(d,n)He^3$ reaction. Deuterium gas targets were used. They consisted of 0.75 atm of D_2 gas contained in a chamber 2.5 cm in length. The entrance window of this chamber was formed from a 1-μm nickel foil. The neutron energy spreads varied from 170 keV at 5 MeV to 70 keV at 7 MeV. The neutron intensity was such that two 1 h runs were needed to get the required number of counts. An additional spectrum was taken for $\frac{1}{5}$th the beam charge with the target cell evacuated in order to determine the intensity and energy of background neutrons from the collimators, Ni foil, and beam catcher.

C. Measurement of Instrumental Effects

Several additional data spectra were accumulated to check on possible instrumental effects. The measurements will be discussed here and the conclusions reached on the basis of these measurements will be discussed in the section on phase-shift analysis. There were a number of possible experimental problems. These were (1) the distortion of the pulse-height spectrum caused by wall effects, (2) the dependence of the phase shifts on the shape of the resolution function, (3) the contribution of recoils due to energy-degraded neutrons produced by inelastic scattering of the primary neutron beam in the brass walls of the scintillator, and (4) events due to disintegrations and recoils caused by the neutron beam in the counter wall coating and in the xenon.

The distortion in the pulse-height distribution due to wall effects can be eliminated by increasing the gas pressure in the counter. However, the cell could not safely contain more than 70 atm, so the wall effect could not be reduced by increasing the pressure. Therefore, instead of increasing the pressure, it was decreased by a factor of 2. A spectrum was taken at 7 MeV and the difference between the phase shifts derived from these data and those derived from the full pressure data was used as a measure of the sensitivity to the wall effect.

The dependence of the phase shifts on the shape assumed for the resolution function was tested by taking additional spectra at 6 and 7 MeV about six months after the original data. During this time lapse the light output of the scintillator had decreased such that the statistical contribution to the energy resolution was greatly increased (R_E became 0.11 whereas it had been 0.04 for 180° recoils at 7 MeV). This produced a truly Gaussian resolution function.

As a check on the contribution from the energy-degraded neutrons produced by inelastic scattering in the cell wall, the amount of brass was increased by a factor of 3.5. This was accomplished by placing a brass sleeve over the cell. Using this configuration, data were taken at the energies where the effect of inelastic events would be most pronounced, i.e., 6 and 7 MeV. The resulting spectra were used to indicate the magnitude of this effect.

The xenon and wall coating background measurements were performed over the entire neutron energy range. It is possible for the incident neutrons to give rise to events in the walls of the counter which in turn cause unwanted events in the gas of the counter. This background is composed of γ rays produced by inelastic scattering in the brass of the cell wall and of recoils and disintegrations caused by neutrons interacting with the coatings on the counter walls or with the xenon.

The xenon is mainly responsible for the γ-ray sensitivity of the counter. Likewise, any wall recoils or disintegrations can be detected by pure xenon alone. Thus, if the helium is removed and only pure xenon is used, the events detected will be those backgrounds mentioned above. However, using pure xenon alone is not feasible since the pulse height produced by a given event can be strongly dependent on the gas mixture and pressure. This makes it impossible to determine how to normalize the background spectrum to the data spectrum in terms of pulse height. So, instead of pure xenon, the cell was filled with the normal amount of xenon, but only a small fraction of the normal amount of helium (2% for energies below 3 MeV and 5% for higher energies). Recoil distributions were then taken using this mixture. The ratio of the background to true recoil

events was thus increased by a factor of either 50 or 20. This means that a distortion of 1% in the normal recoil spectrum could appear as a 50 or 20% distortion in the background spectrum.

IV. CONVERSION OF ENERGY DISTRIBUTIONS TO RELATIVE CROSS SECTIONS

A. General

The process of deriving cross sections from the recoil energy distributions involved the removal of a number of instrumental effects. First, the pulse-height distributions were corrected for the baseline displacement of the electronics associated with the linear signal. After this was done, the relation between the pulse height and recoil energy which was previously mentioned was used to assign a recoil energy to each channel in the recoil spectrum. This relation was also used to correct the spectrum for the effects of differential nonlinearity.

The spectra were then corrected for the effects of double scattering from the helium in the counter. These corrections were calculated using a random-walk procedure and cross sections calculated from the DGS phase shifts. The corrections were smeared by the energy resolution of the counter before they were applied to the data spectrum. Greater detail on this correction can be found in Ref. 13.

After the above corrections were completed, the spectra were fit using a computer code which (1) normalized the pulse-height axis of the spectrum to a scale proportional to $\cos\theta$, where θ is the center-of-mass scattering angle, (2) removed the effects of the finite energy resolution, and (3) extracted the coefficients of a cosine series expansion for the true differential cross section.

B. Fitting the Recoil Spectra

The angular normalization of the recoil spectra and the removal of resolution effects are closely related and were accomplished simultaneously. The effect of the finite energy resolution on the helium recoil pulse-height distribution is illustrated in Fig. 5. The solid curve is the differential cross section at 1 MeV calculated from the DGS phase shifts. If the energy resolution of the counter were perfect, this curve would also represent the pulse-height distribution. The dashed curve shows the pulse-height distribution which would result for an energy resolution of Gaussian shape, having the energy dependence discussed previously. The resolution for the α-particle energy produced by 180° scattering is 0.14.

In Sec. II A, a relation for the energy dependence of the resolution is given. This information is actually based in a large way on the analysis of the recoil spectra reported here. In fact, for a particular He scintillator, there was no way to predetermine the

[13] G. L. Morgan, thesis, Duke University, 1967 (unpublished).

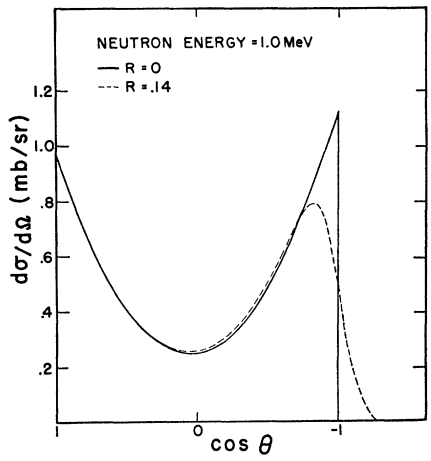

FIG. 5. Illustration of the effects on the helium recoil spectra of the finite energy resolution of the counter.

magnitude of R_v and R_E. Therefore, R as well as the channel in the pulse-height spectrum which corresponded to 180° scattering were initially treated as adjustable parameters in a fit to the spectrum. Further investigation of the R's led to the conclusions in Sec. II A and Ref. 9.

The differential cross section can be written as a cosine series,

$$k^2\sigma(\cos\theta)=\sum_{N=0}^{2l_{\max}} A_N \cos^N\theta,$$

where $l_{\max}$ is the highest partial wave which contributes to the interaction. This can be rewritten as

$$k^2\sigma(y)=\sum A_N y^N, \qquad y=\cos\theta=1-2E_a/E_{a\max}, \quad (2)$$

where E_a is the helium recoil energy for scattering at an angle θ, and $E_{a\max}$ is the maximum helium recoil energy (for 180° scattering).

If the energy resolution of the cell were perfect, then Eq. (2) would also give the relative pulse-height distribution

$$N(x)=k^2\sigma(x)=\sum A_N x^N.$$

But for finite resolution this expression must be modified. It becomes

$$N(x)=k^2\int_{y(0°)}^{y(180°)} \sigma(y)K(x,y)dy,$$

where the kernel represents the effects of the resolution of the cell. Using Eq. (2) this can be written

$$N(x)=\int \sum A_N y^N K(x,y)dy$$

$$=\sum A_N \int y^N K(x,y)dy$$

$$=\sum A_N G_N(x), \quad (3)$$

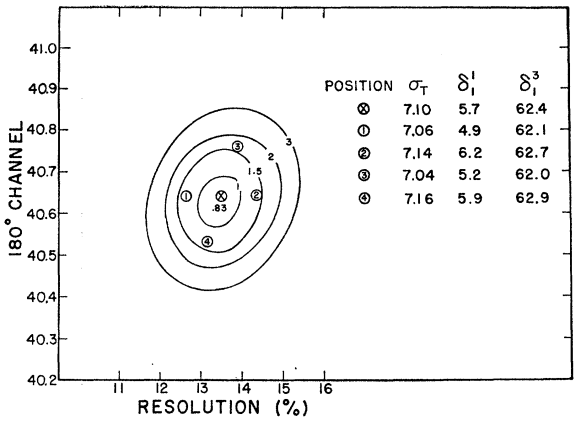

FIG. 6. Contour map of the error of the fit to the 1-MeV distribution. The table refers to the values obtained for the phase shifts for fits resulting in several values of the fitting error.

where

$$G_N(x)=\int_{y(0°)}^{y(180°)} y^N K(x,y)dy.$$

In the present experiment, the resolution function was assumed to be Gaussian. Therefore,

$$K(x,y)=[a/(1-y)R(y)]\times\exp[-b(x-y)^2/(1-y)^2R^2(y)],$$

where

$$a=2.355(2\pi)^{-1/2} \quad \text{and} \quad b=(2.355)^2/2.$$

Here a and b are normalization constants and $R(y)$ is the value of the resolution for recoil energies corresponding to scattering through an angle given by $\cos\theta=y$. $R(y)$ was chosen to have the energy dependence discussed earlier,

$$R(y)=\{R_v^2+R_s^2/E_a\}^{1/2}=\{R_v^2+R_s^2/[0.5(1-y)E_{a_{\max}}]\}^{1/2}.$$

Since Eq. (3) is a linear form, the coefficients A_N can be found by a least-squares fit to the data once the $G_N(x)$ are calculated. A guess was made as to which channel number represented the 180° scattering point. The pulse-height spectrum was normalized to this choice. This determined the value of x for each channel number. A resolution was chosen and the G_N were calculated. The least-squares fit then provided the A_N. Using these A_N and the G_N, a calculated spectrum was formed and an error quantity of the form

$$\chi^2=\frac{1}{n}\sum_{k=1}^{n}[N_k^{\text{expt}}(x_k)-N_k^{\text{calc}}(x_k)]^2/[\Delta N_k(x_k)]^2$$

was calculated. The superscripts "expt" and "calc" refer to the experimental and calculated values at the pulse height x_k. The number of data points is given by n. $\Delta N(x_k)$ is the experimental uncertainty for the number of counts at pulse height x_k and was taken to be the value due to the statistical accuracy associated with the number of counts in that channel, account being taken of any background present.

These calculations were made using a computer which had the capability for display on an oscilloscope.

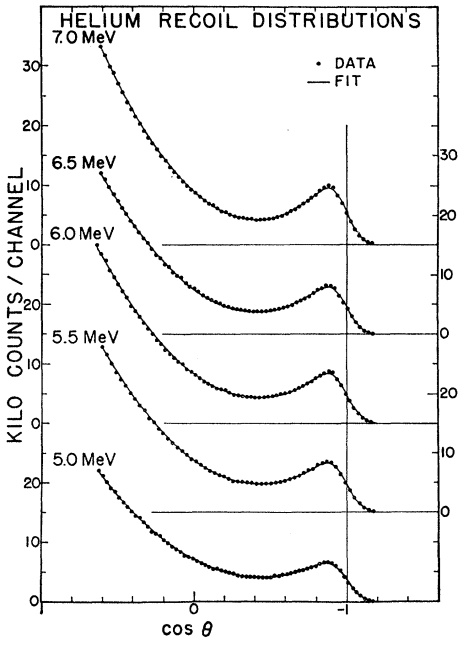

FIG. 7. Helium recoil distributions for neutron energies from 5.0 to 7.0 MeV.

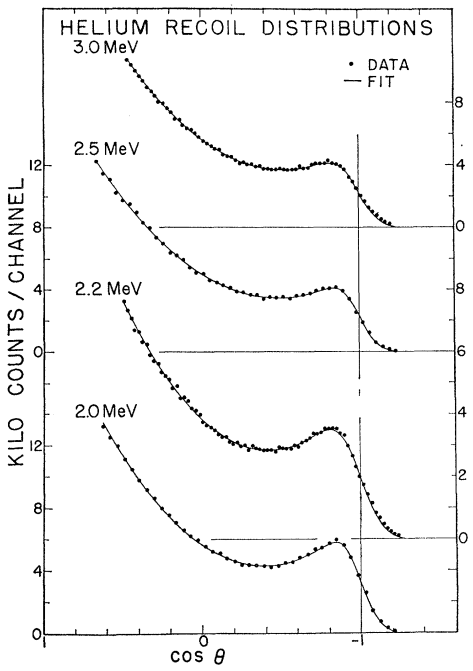

FIG. 8. Helium recoil distributions for neutron energies from 2.0 to 3.0 MeV.

After the calculation was performed, the data curve and the fitted curve were displayed on the oscilloscope. After comparing the two curves, the resolution and/or normalization was adjusted and the calculation repeated. In this way the values of the resolution and normalization which gave the smallest error could be quickly found.

A contour map of the error versus resolution and the channel number for 180° scattering is shown in Fig. 6. The neutron energy was 1.0 MeV. As can be seen there is a well-defined minimum in the error surface. To check on how the values of resolution and relative normalization affected the phase shifts derived from the data, phase shifts were calculated (using a method to be discussed later) for a number of positions on the error surface shown in Fig. 6. The points chosen represent

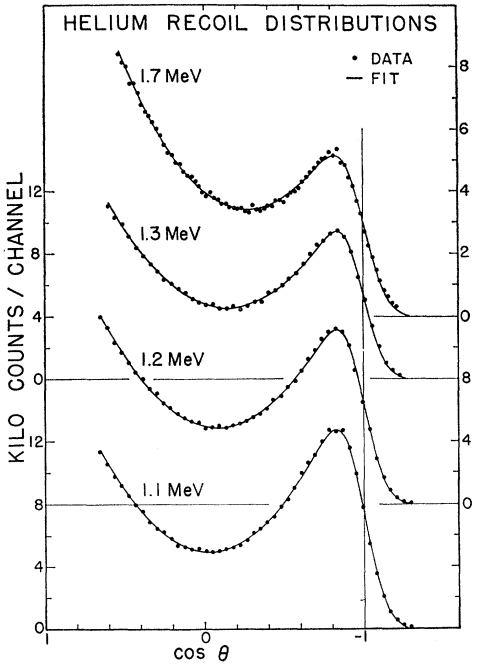

FIG. 9. Helium recoil distributions for neutron energies from 1.1 to 1.7 MeV.

values of the error which are about twice the value at the minimum. The results are shown in the table in Fig. 6. It was found that at all points the phase shifts agreed with the values found at the minimum to within 0.5°. The results at 1.0 MeV are about average; the minimum in the error was sharper at the high energies (5 to 7 MeV) but less sharp around 2.5 MeV and below 0.5 MeV.

In order to further ensure that the method of analysis was reliable, the resolution and relative normalization were required to vary in a smooth way with neutron energy. At all energies, a value of 8% was used for the volume contribution to the resolution (R_v).

The helium recoil spectra recorded in the course of this investigation are shown in Figures 7 to 11. The

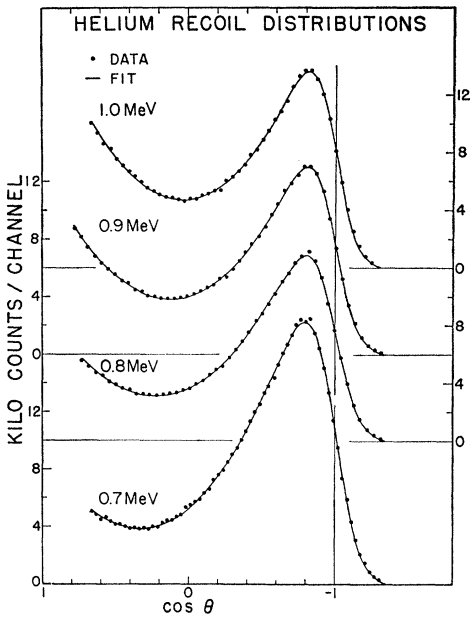

FIG. 10. Helium recoil distributions for neutron energies from 0.7 to 1.0 MeV.

solid curves are the fits discussed above. At the lower energies (3 MeV and below) the average value of the error of the fit was about 1.0. From 5 to 7 MeV this average value was about 2.4. There are two reasons for the greater error at the higher energy. Firstly, as discussed in the section on the resolution study, the approximation of a Gaussian shape for the resolution was not strictly correct at the higher energies. Later data taken at these energies with the resolution purposely

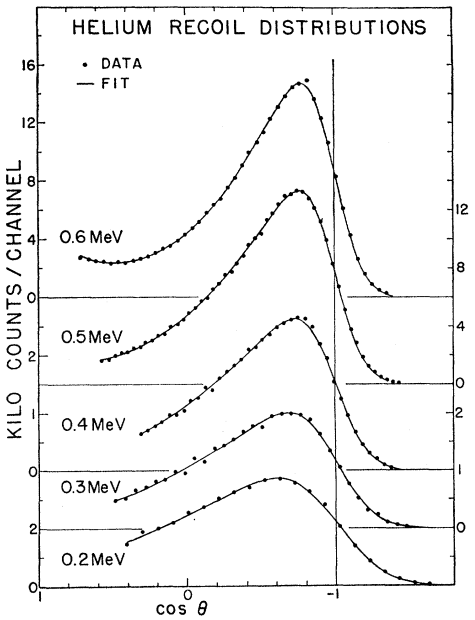

FIG. 11. Helium recoil distributions for neutron energies from 0.2 to 0.6 MeV.

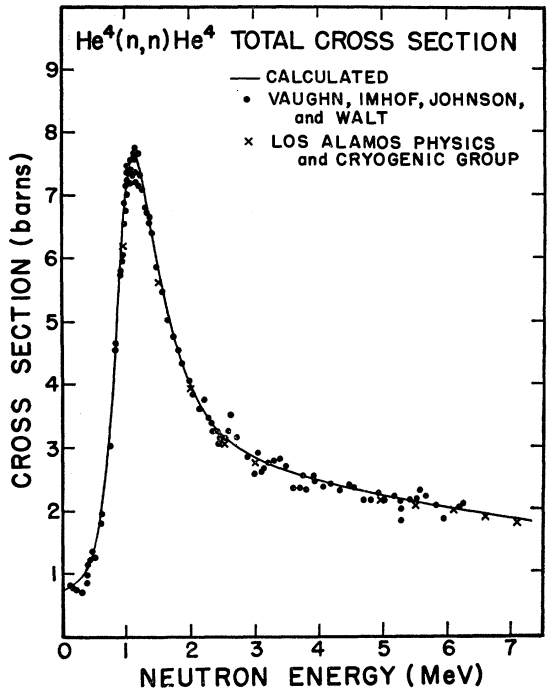

FIG. 12. Comparison of calculated total cross section to the experimental values.

made poorer and with the same counting statistics gave an error of about 1.5. Secondly, the number of counts per channel was very large (20 000 to 30 000 in the lower channels), making the statistical error small and thus amplifying the presence of any unaccounted-for experimental errors.

The fits were made assuming that only s and p waves contribute to the interaction, i.e., $l_{\max}=1$. While the assumption of no d-wave interaction below 3 MeV seemed valid, there might be small d-wave contributions in the energy range from 5 to 7 MeV. As a test, fits were made to the higher-energy data assuming that d waves were present, that is, fitting with terms up to the fourth power in the cosine series. The error of these fits was not significantly smaller than the fits allowing s and p waves only. It was thus concluded that the data can be satisfactorily represented without considering partial waves higher than p waves. This agrees with the conclusions of Hoop and Barschall.[7]

V. PHASE-SHIFT ANALYSIS

A. Calculation of the Phase Shifts

The cross-section expansion coefficients A_N contain all the information about the scattering at any given energy; thus the phase shifts could be determined directly from these quantities. Pisent[14] has described a method for calculation of the phase shifts from the expansion coefficients. For the case where only s and p waves contribute to the interaction, the calculation results in the eight possible sets of phase shifts which will lead to the same cross section. In the neutron-helium case the correct solution was easily determined on the basis of other data.

Because the measurements of the present work were only relative distributions, the A_N derived from fitting the pulse-height spectra were undetermined to within a multiplicative constant. The coefficients could be normalized using the experimental values of the total cross section, but these values were not sufficiently accurate to be of use as the primary normalization standard. An alternative normalization procedure was adopted whereby the s-wave phase shift was determined in advance. The total cross section was then chosen such that when the coefficients were normalized to that value, the s-wave phase shift calculated from the coefficients had its assigned value. Since the previously existing experimental data indicate that the s-wave phase shift is consistent with that due to scattering from a hard sphere, in the present analysis the s-wave phase shift was assigned a value given by

$$\delta_0{}^1=\pi-kR_0,$$

where k is the wave number and R_0 is the hard-sphere radius.

The data of Sawers *et al.*,[1] that of Hoop and Barschall,[7] and the thermal neutron cross section[15] are all consistent with values of the hard-sphere radius R_0 between 2.4 and 2.5 F. The value used in the present work was 2.44 F. The reason for choosing this value is discussed in more detail below.

Usually there existed more than one discrete value of the total cross section which would lead to the specified s-wave phase shift. However, in all cases there was only one value which was compatible with the existing total cross-section measurements. After the correct total cross section was found, the p-wave phase shifts were calculated using the same normalization. These phase shifts are given in Table I. The total cross sections obtained from the analysis are compared to the measured values[15] in Fig. 12.

The phase shifts are very sensitive to the expansion coefficients in the energy region where the $P_{3/2}$ phase shift passes through 90° (1.25-MeV neutron energy). This phenomenon is evidenced by the scatter in the p-wave phase shifts at 1.2 and 1.3 MeV. When phase shifts at 1.2 and 1.3 MeV were interpolated from the surrounding energies by means of a resonance fit, the cross sections calculated from these phase shifts agreed with the measured cross sections to within less than 1% at all angles.

[14] G. Pisent, Helv. Phys. Acta **36**, 248 (1963).

[15] *Brookhaven National Laboratory Report No. 325, Suppl.* 2, compiled by J. R. Stehn, M. D. Goldberg, B. A. Magurno, and R. Wiener-Chasman (U. S. Government Printing Office, Washington, D. C., 1964).

B. Tests of Instrumental Effects

The recoil spectra taken to test various instrumental effects were also analyzed to obtain phase shifts. The spectrum taken at 7 MeV with one-half the normal pressure in the counter gave phase shifts which were in agreement with the full pressure data to within about 1°, thus indicating that wall effects could be neglected.

Likewise, the spectra at 6 and 7 MeV which were obtained with intentionally poorer resolution reproduced the earlier phase shifts to within 1°. The deviation from the original phase shifts was not systematic and was ascribed to the inherent experimental uncertainty rather than the difference in resolution function shapes.

A further investigation of the dependence of the phase shifts on the resolution function was made at a number of energies. The study of the resolution function had indicated that the shape of this function might not be symmetric. To test the sensitivity of the phase shifts to this feature, fits were made to several spectra using a resolution function which was asymmetric, each side having a Gaussian shape. In general, the fits were slightly better, but it was not clear whether this was due to a real improvement in the representation of the resolution effect or due to the addition of an extra parameter in the fit. Asymmetries (ratio of the half-width of the higher side of the Gaussian to the half-width of the lower side) on the order of 1.05 to 1.20 were used. The phase shifts obtained from these fits were the same as were obtained with a symmetric Gaussian resolution to within a few tenths of a degree.

There was some evidence from the spectra taken at 6 and 7 MeV with the extra brass around the counter that there was a contribution from the inelastic scattering in the brass. A definite background was present in the lowest usable channels (channels 12 to 18 out of 80). The contribution (about 2%) caused a factor-of-2 increase in the error of the fit and at both energies the p-wave phase shifts were about 2° higher than those derived from the measurements taken without extra brass. However, if the lowest six channels were deleted from the fit, both the error and the phase shifts were in good agreement with the original data. To test this effect in the original data, the spectra taken with the normal amount of brass were refitted with the lowest six channels deleted. There was little change in the error of the fit and the phase shifts did not change. Since the increase in the amount of brass was large (350%) and the background contribution was confined to the lowest channels, the effect on the original data of the counter walls must have been quite small and thus the effect was neglected.

The recoil spectra obtained with a small fraction of the normal helium pressure were examined for evidence of backgrounds. Although the small helium pressure had prevented accumulation of good counting statistics, the measurements were of sufficient accuracy to show that any contribution to the full-pressure pulse-height spectrum associated with spurious events was small enough to be neglected, i.e., less than 1% at all pulse heights used in the fits.

TABLE I. Cross-section expansion coefficients and phase shifts.

E_n (MeV)	A_0	A_1	A_2	σ_T (b)	$\delta_0{}^1$ (deg)	$\delta_1{}^1$ (deg)	$\delta_1{}^3$ (deg)
0.202	0.0379	−0.0338	0.0094	0.828	169.0	0.5	2.8
0.303	0.0584	−0.0788	0.0274	0.909	166.5	0.9	4.6
0.402	0.0826	−0.1349	0.0632	1.052	164.5	1.2	7.2
0.501	0.1236	−0.2319	0.1628	1.448	162.7	1.4	12.2
0.599	0.1810	−0.3561	0.3896	2.116	161.1	2.6	18.6
0.704	0.2831	−0.4568	0.7086	3.008	159.5	2.8	26.4
0.799	0.4028	−0.5143	1.1888	4.078	158.1	4.0	34.9
0.899	0.6197	−0.4394	1.8834	5.658	156.8	4.5	47.5
1.008	0.8736	−0.1449	2.6559	7.115	155.4	5.8	62.5
1.106	1.0541	0.2293	3.0374	7.619	154.2	6.5	74.9
1.207	1.1710	0.6056	3.0967	7.443	153.1	6.0	85.4
1.306	1.2131	0.9424	3.0533	6.965	152.0	13.5	98.6
1.700	1.2593	1.4119	2.4384	4.970	148.0	12.7	111.0
1.961	1.2615	1.5765	2.0068	4.014	145.7	14.6	118.4
2.200	1.3100	1.6721	1.9552	3.636	143.7	17.7	119.4
2.454	1.3468	1.7553	1.7825	3.225	141.6	21.0	122.4
2.980	1.4454	1.9610	1.8511	2.822	137.7	28.8	123.9
5.028	1.5759	3.0963	3.5108	2.227	125.0	46.1	118.1
5.505	1.5702	3.3610	3.8880	2.123	122.5	49.6	117.4
5.988	1.5634	3.6049	4.2621	2.032	120.0	51.3	115.7
6.523	1.5633	3.8325	4.5725	1.930	117.4	52.1	113.7
7.013	1.5593	4.0318	4.8418	1.845	115.0	53.0	112.2

Some qualifications should be made for the very-low-energy phase shifts. The counter linearity measurements were only conducted down to 0.2 MeV neutron energy, so the linearity corrections to the entire 0.2-MeV spectrum and to large portions of the 0.3- and 0.4-MeV spectra were based on an extrapolation of the linearity data to lower energies. This, combined with the facts that the forward-angle cross sections are very small and the resolution is poor (about 20% for 180° recoils at 0.2 MeV), produces a fairly large uncertainty in these lowest energies. However, the phase shifts found here seem to be in good agreement with an extrapolation of the higher-energy data and are believed to be correct to within 1° or 2°. The total cross sections determined in this region are not in good agreement with the experimental values, but it is difficult to estimate the error on the experimental values. Judging from the point scatter in the published data, this error at 0.4 MeV could be as large as 20%.

VI. FITS TO A RESONANCE FORMULA

A. General

The p-wave phase shifts derived from the data were fitted with a single-level resonance formula. The single-level dispersion theory as described by Lane and Thomas[16] was employed in this analysis. While there was little new information to be gained from such fits, they did serve a number of useful purposes. The phase-shift curves generated by the fits provide smooth,

[16] A. M. Lane and R. G. Thomas, Rev. Mod. Phys. **30**, 257 (1958).

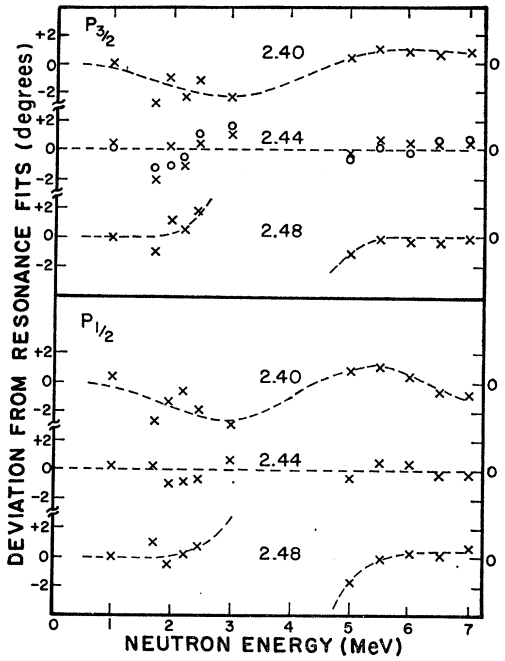

FIG. 13. Illustration of the dependence of the quality of the resonance fits on the choice of the s-wave hard-sphere radius used to normalize the cross-section data. The circles for the plot of the $P_{3/2}$ phase shift at 2.44 F indicate the deviation from a fit when the background contribution discussed in Sec. VII was included. The corresponding points are not shown for the $P_{1/2}$ phase shift because there was no noticeable difference from the values obtained without background.

continuous curves through the data points, thus providing a means of smoothing out the random deviations in the data and allowing interpolation of the phase shifts at energies other than those where the data was available. Also, assuming that the single-level approximation is a good one, the resonance formula should accurately describe the energy variation of the p-wave phase shifts and thus provide a means of determining what the best value for the s-wave hard-sphere radius should be.

B. Single-Level Formulas

The principal parameters in the theory are the characteristic energy of the level $E_{\lambda l}{}^J$, the reduced width $\gamma_{\lambda Jl}{}^2$, the interaction radius A, and the boundary condition by which the radial part of the internal wave functions $r^{-1}u(r)$ are defined. This definition is given by

$$\left[\frac{r}{u_\lambda(r)}\frac{d}{dr}u_\lambda(r)\right]_{r=A}=B.$$

For the choice $B=0$, the R function is easily related to the logarithmic derivative at the radius A,

$$R_l{}^J=1/Y_l{}^J,$$

where $Y_l{}^J$ is the logarithmic derivative of the wave function in the state of total angular momentum J and orbital angular momentum l. In the single-level approximation $R_l{}^J$ can be expressed as

$$R_l{}^J=\gamma_{\lambda Jl}{}^2/(E_{\lambda l}{}^J-E),$$

where E is the energy of the system. Thus $Y_l{}^J$ is given by

$$Y_l{}^J=(1/\gamma_{\lambda Jl}{}^2)(E_{\lambda l}{}^J-E).$$

If A is greater than the range of interaction, the $Y_l{}^J$ can be evaluated at each energy where the phase shifts are known by means of the relation

$$Y_l{}^J=\frac{F_l'(\rho)+G_l'(\rho)\tan\delta_l{}^{2J}}{F_l(\rho)+G_l(\rho)\tan\delta_l{}^{2J}},$$

where $\delta_l{}^{2J}$ is the phase shift describing the interaction in the state of orbital angular momentum l and total angular momentum J. Here ρ is the product kr and $F_l(\rho)$ and $G_l(\rho)$ are the free-particle wave functions for orbital angular momentum l, with the primes denoting differentiation with respect to ρ. Thus, for a set of phase shifts $\delta_l{}^{2J}(E)$, a simple least-squares fit of $Y_l{}^J$ with respect to E will yield values of $\gamma_{\lambda Jl}{}^2$ and $E_{\lambda l}{}^J$ for the boundary value $B=0$.

C. Dependence of Fit on Hard-Sphere Radius

As mentioned previously, the choice of 2.44 F for the s-wave hard-sphere radius was made on the basis of

TABLE II. Phase shifts calculated from resonance parameters.

E_n (MeV)	$\delta_0{}'$ (deg)	$\delta_1{}^1$ (deg)	$\delta_1{}^3$ (deg)	$\delta_0{}^1$ (deg)	$\delta_1{}^1$ (deg)	$\delta_1{}^3$ (deg)
0.10	172.3	0.2	0.7	172.0	0.1	0.7
0.20	169.0	0.5	2.1	168.8	0.4	2.1
0.40	164.5	1.3	7.4	164.1	1.1	7.4
0.60	161.0	2.4	17.5	160.6	2.1	17.5
0.80	158.1	3.8	35.4	157.6	3.3	35.4
1.00	155.5	5.4	61.1	155.0	4.7	61.0
1.20	153.2	7.2	85.2	152.6	6.3	85.1
1.40	151.0	9.2	101.0	150.5	8.1	101.0
1.60	149.0	11.3	110.1	148.5	10.0	110.3
1.80	147.1	13.6	115.5	146.6	12.1	115.7
2.00	145.3	16.0	118.7	144.8	14.2	119.0
2.20	143.6	18.4	120.6	143.2	16.5	121.0
2.40	142.0	20.9	121.8	141.6	18.8	122.3
2.60	140.5	23.4	122.4	140.1	21.2	123.0
2.80	139.0	25.8	122.8	138.6	23.6	123.4
3.00	137.5	28.3	122.8	137.2	26.1	123.6
3.50	134.1	34.0	122.3	134.0	32.0	123.3
4.00	131.0	38.9	121.2	131.0	37.5	122.5
4.50	128.0	43.1	119.8	128.2	42.3	121.4
5.00	125.2	46.4	118.3	125.6	46.4	120.1
5.50	122.5	49.0	116.7	123.2	49.9	118.8
6.00	119.9	50.9	115.1	120.9	52.6	117.5
6.50	117.5	52.3	113.4	118.8	54.9	116.1
7.00	115.1	53.3	111.7	116.8	56.6	114.8
7.50				114.8	57.9	113.5
8.00				113.0	58.9	112.2
9.00				10.97	60.1	109.7
10.00				106.7	60.6	107.2
11.00				104.0	60.5	105.0
12.00				101.7	60.2	102.8
13.00				99.6	59.5	100.7
14.00				97.8	58.7	98.8
15.00				96.3	57.8	96.9
17.00				94.0	55.8	93.5
19.00				92.9	53.7	90.4

the quality of the resonance fits. p-wave phase shifts were calculated from the expansion coefficients normalized on the basis of s-wave hard-sphere radii of 2.40, 2.44, and 2.48 F. Resonance fits were made to each set of phase shifts. The resulting fits indicated that a value of 2.44 F for the hard-sphere radius gave p-wave phase shifts which were most consistent with the resonance formula. This is illustrated in Fig. 13, which shows the deviation of the experimental phase shifts from the values obtained from resonance fits to each set. The very-low-energy data is not shown, as it was not sensitive to the choice of hard-sphere radius. The fit for 2.40 F shows a systematic deviation from the data. At 2.44 F the average deviation is smaller and has a more random character. For a hard-sphere radius of 2.48 F the fit for energies below 2.5 and above 5.5 MeV is about as good as that for 2.44 F. However, there is no solution for the p-wave phase shifts at 2.98 MeV for a hard-sphere radius of 2.48 F. (That is, certain mathematical conditions necessary for the existence of real phase shifts are not satisfied when the coefficients are normalized to give the s-wave phase shift required by a hard-sphere radius of 2.48 F.) The p-wave phase shifts for a hard-sphere radius of 2.46 F show a large deviation at 2.98 MeV from the fitted curves. It was also found that for a hard-sphere radius of 2.50 F solutions did not exist at a number of energies in the vicinity of 3.0 MeV. This tendency is indicated by the dashed line for the fits at 2.48 F in Fig. 13.

Resonance fits to the phase shifts listed in Table I ($R_0=2.44$ F) are shown in Fig. 14. The fit is good and so the single-level formula provides a means of calculating the phase shifts at any given energy in this range. The fits were made at an interaction radius of $A=3.0$ F, with the boundary condition $B=0$. The resulting parameters are

$$E_\lambda(P_{3/2})=-4.93 \text{ MeV}, \quad \gamma_\lambda^2(P_{3/2})=7.89 \text{ MeV},$$
$$E_\lambda(P_{1/2})=1.97 \text{ MeV}, \quad \gamma_\lambda^2(P_{1/2})=23.05 \text{ MeV}.$$

It should perhaps be noted that the choice of boundary condition was not the optimum for obtaining information about the compound state.[16] However, this boundary condition is the most convenient for calculating phase shifts and the values of the parameters resulting from other choices of B are easily calculated from the parameters given above. The fits to the data are independent of B.

TABLE III. Polarization data of May, Walter, and Barschall at 6.0 MeV.

θ_{lab} (deg)	ϵ	$\delta P(\theta,\phi)$	ϵ_{corr}	$\Delta\epsilon$	P_2 [a]	ΔP_2 [a]
30	0.077	0.001	0.078	0.012	−0.390	0.060
40	0.088	0.002	0.090	0.013	−0.450	0.065
50	0.135	0.004	0.139	0.010	−0.695	0.050
60	0.136	0.005	0.141	0.011	−0.705	0.055
70	0.150	0.006	0.156	0.020	−0.780	0.100
80	0.145	0.004	0.149	0.014	−0.745	0.070
90	0.087	−0.005	0.082	0.021	−0.410	0.105
100	−0.082	−0.013	−0.095	0.015	0.475	0.075
110	−0.159	−0.014	−0.173	0.014	0.865	0.070
120	−0.184	−0.007	−0.191	0.014	0.955	0.070

[a] Assuming $P_1=-0.200$.

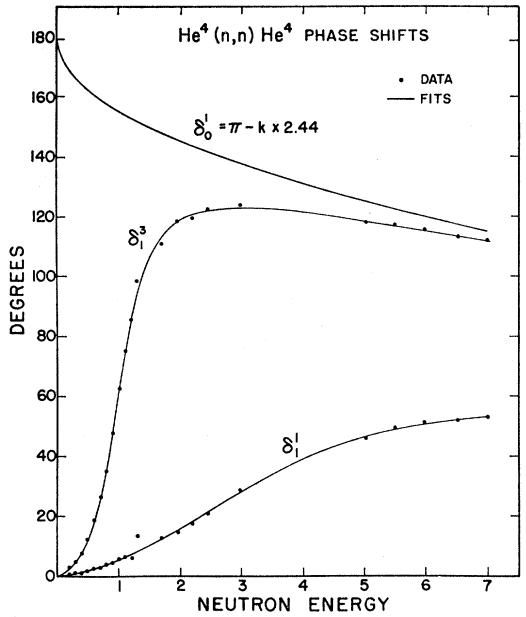

FIG. 14. Resonance fits to the p-wave phase shifts. The dots represent the experimental values while the curves are the results of the fits. Note that the s-wave phase shift is shown as the curve of hard-sphere values.

In Table II phase shifts are given in column 2 for the s wave calculated for a hard-sphere radius of 2.44 F and in columns 3 and 4 for the p waves calculated with the above resonance parameters.

VII. PREVIOUS EXPERIMENTAL INFORMATION

The set of neutron-helium phase shifts of most recent origin is that published by Hoop and Barschall.[7] Below 8.0 MeV this set of phase shifts is very close to the DGS phase shifts. Other experimental information of recent origin is the data reported in the previous paper[1] and the data reported by May *et al.*[6] The latter work included measurements of the angular dependence of the polarization at 2.0 and 6.0 MeV. The phase shifts derived from the 2.0-MeV data are discussed in the previous paper. For the work reported here similar corrections were calculated and the same analysis was made of the data at 6.0 MeV. The only correction of significance was the $\delta P(\theta,\varphi)$ for the finite size of the scintillators. Table III lists the values obtained. The notation is the same as in Ref. 1.

The comparison of the present phase shifts with those mentioned above is illustrated in Fig. 15. The curves are the resonance fits to the present phase shifts, i.e., the same curves as are shown in Fig. 14. The HB phase

shifts are represented by the solid triangles. For the S and $P_{3/2}$ phase shifts, agreement with the present values is good over the whole energy range, but such is not the case for the $P_{1/2}$ phase shift. Above 2 MeV, there is a gradually increasing difference between the two sets of phase shifts. This disagreement is not too surprising since the HB $P_{1/2}$ phase shift was taken to be the DGS values without any modification for energies below 6 MeV.

The phase shifts obtained by Sawers *et al.* are shown as the open circles in Fig. 15. At 2.44 MeV agreement with the present work is quite good. The analysis by Sawers *et al.* of the May *et al.* data at 2.0 MeV also yielded phase shifts in good agreement with the present work. At 1.0 MeV agreement is good for the S and $P_{3/2}$ phase shift, but there is a 1° difference in the $P_{1/2}$ phase shift.

The analysis of the data of May *et al.* was performed in a manner similar to that of Sawers *et al.*[1] at 2.44 MeV. The χ^2 was a minimum for $\delta_0{}^1=121°(\pm4°)$, $\delta_1{}^1=56°$ $(\pm5°)$, $\delta_1{}^3=119°(\pm4°)$, and $P_1=-0.200(\pm0.012)$. The values in the parentheses represent the changes when χ^2 takes on a value 1.5 times the minimum χ^2, all four quantities being considered as free parameters in the search. While the agreement between these phase shifts and the present values is not particularly good, they are consistent. It should also be noted that the inclusion of d waves in the fit to the 6.0-MeV data did not appreciably decrease the χ^2 of the fit, thus indicating that d waves were not necessary. This conclusion is in agreement with the analysis of HB and with the present analysis of the cross-section data.

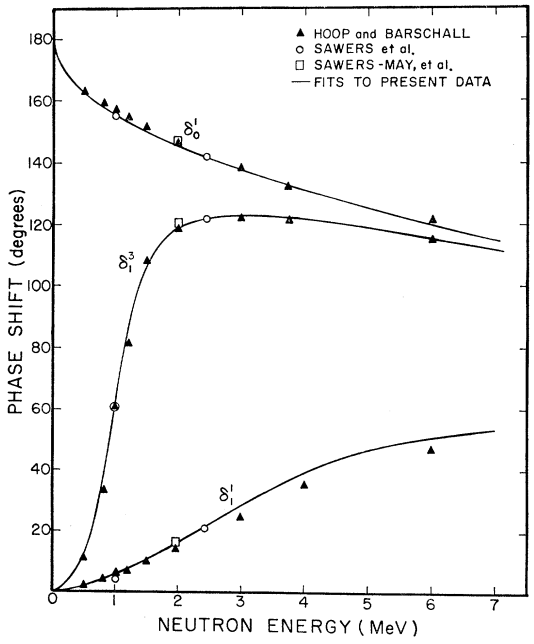

FIG. 15. Comparison of present phase shifts to the previous experimental data. The curves are the same ones which appear in Fig. 14 and represent the present phase shifts.

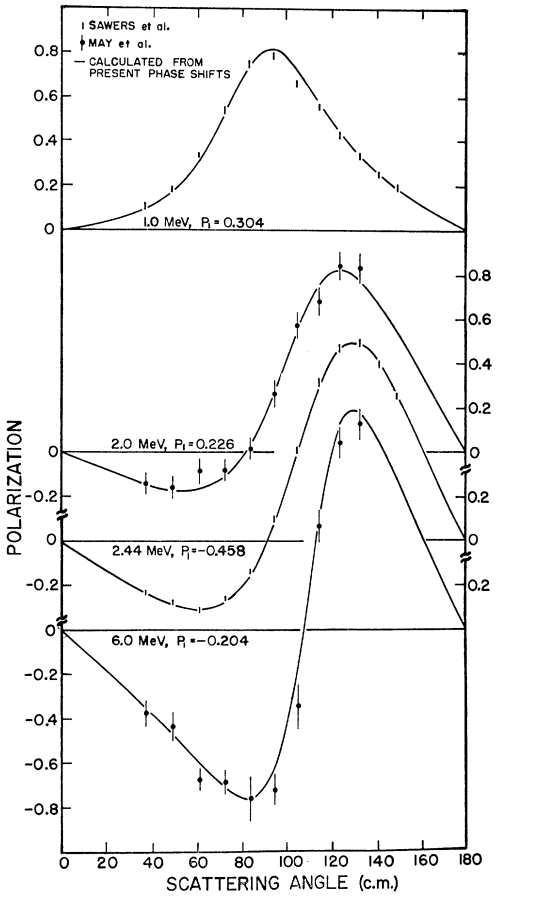

FIG. 16. Comparison of the polarizations calculated from the present phase shifts to the experimental data. The experimental data has been normalized for best agreement.

In addition to comparison of phase shifts, the polarizations calculated from the present (single-level) phase shifts were compared directly to the data. This is shown in Fig. 16. At each energy the polarization P_1 was adjusted for best agreement. Note that at 1.01, 2.0, and 2.44 MeV the values of P_1 were the same as those determined by Sawers *et al.* (The present phase shifts favored the lower limit of the 1.015±0.007 MeV quoted by Sawers *et al.* The comparison in Fig. 16 was made, in fact, assuming the energy to be 1.008 MeV.) At 6.0 MeV, P_1 is slightly different from that value determined in the analysis mentioned above (−0.205 versus −0.200).

An investigation was also made to determine how well the present phase shifts could be connected to the HB phase shifts for the higher energies. It was found that while the two sets of phase shifts could be connected by smooth curves, an extrapolation of the present phase shifts by means of the resonance parameters was not in agreement with the HB phase shifts at energies above 8 MeV. A single-level resonance fit using the present phase shifts below 8 MeV and the HB phase shifts from 8 to 18 MeV also failed to give satisfactory agreement. However, if allowance was made for a

background contribution in the p-wave resonance fits, good agreement could be obtained from 1 to 18 MeV. The fits were only mildly sensitive to the value given the background; the values used were calculated on the basis of single-particle states at energies of about 200 MeV and having reduced widths of 60 MeV. (Reasons for this particular choice are given in the next section.) The resulting fits which are shown in Fig. 17 indicate that the present phase shifts connect onto those of HB fairly well. In columns 5, 6, and 7 in Table II, we list phase shifts from the curves in Fig. 17. The level parameters in this case are

$$E_\lambda(P_{3/2}) = -6.24 \text{ MeV}, \quad \gamma_\lambda^2(P_{3/2}) = 11.83 \text{ MeV},$$
$$E_\lambda(P_{1/2}) = 2.76 \text{ MeV}, \quad \gamma_\lambda^2(P_{1/2}) = 14.22 \text{ MeV},$$

and $B=0$, $A=3.0$ F. Below 7 MeV, the hard-sphere values for $\delta_0{}^1$ (column 2 in Table II) do not differ appreciably from the values given by the single-level fit to the s-wave phase shifts (column 4 in Table II). For the latter case, the resonance parameters $[E_\lambda(S_{1/2}) = 24.8$ MeV and $\gamma_\lambda^2(S_{1/2}) = 4.1$ MeV] are of no significance, but such a fit provides a convenient means of drawing a smooth curve through the data up to 18 MeV.

VIII. COMPARISON TO PROTON-HELIUM SCATTERING

It was felt that a comparison of the neutron-helium phase shifts to the proton-helium phase shifts would be of interest. For this comparison a set of proton-helium phase shifts were calculated from the neutron data. The resonance parameters which were obtained from the fits shown in Fig. 17 were used for this calculation. The reduced widths were taken to be the same for both He^5 and Li^5. The characteristic energies were shifted by 1.5 MeV to bring into agreement the phase shifts near the $P_{3/2}$ resonance in Li^5. Phase shifts were calculated up to 100 MeV using the p-wave background parameters given above.

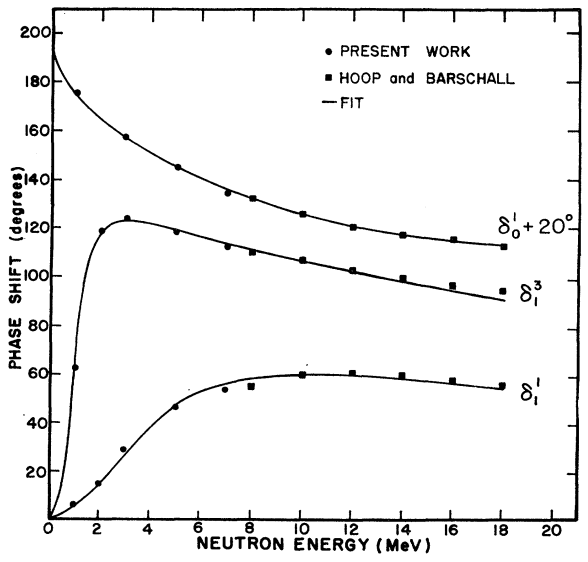

FIG. 17. Resonance fits to neutron-helium data from 1 to 18 MeV. The p-wave fits include the background contribution discussed in Sec. VII.

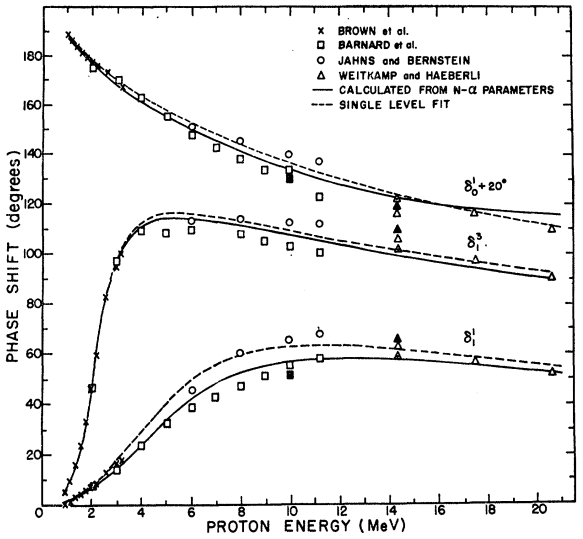

FIG. 18. Proton-helium phase shifts. The solid curve is calculated on the basis of the neutron-helium resonance parameters of the curves shown in Fig. 17. The dashed curves are resonance fits to the proton-helium phase shifts. Background contributions are included for the p-wave fits.

These phase shifts are compared to the experimental values in Fig. 18. The solid curves are the values calculated from the neutron data. The experimental data are shown by the crosses, squares, circles, and triangles. These are the data of Brown *et al.*,[17] Barnard *et al.*,[18] Jahns and Bernstein,[19] and Weitkamp and Haeberli,[8] respectively. Also shown for comparison is a resonance fit to the proton data. This is the dashed curve in Fig. 18. Allowance was made for a background contribution in the p-wave fits. The data of Barnard *et al.* were not considered in making these fits since Jahns and Bernstein had made use of the cross-section data of Barnard *et al.* in deriving their phase shifts.

From 20–60 MeV, recent data of Boschitz *et al.*[20] are available along with preliminary phase shifts. These phase shifts were employed to determine the background resonance parameters in the p waves. The single-level (with background) calculation for proton-helium scattering have $P_{1/2}$ phase shifts of 50° and 40° at 25 and 50 MeV, respectively, compared with the values of around 47° and 42° from Ref. 20. Similarly, the $P_{3/2}$ values are 89° and 69° compared with values

[17] L. Brown, W. Haeberli, and W. Trachslin, Nucl. Phys. **A90**, 339 (1967).
[18] A. C. L. Barnard, C. M. Jones, and J. L. Weil, Nucl. Phys. **50**, 604 (1964).
[19] M. F. Jahns and E. M. Bernstein, Phys. Rev. **162**, 871 (1967).
[20] E. T. Boschitz, M. Chabre, M. E. Conzett, H. E. Shield, and R. J. Slobodrian, in *Proceedings of the 2nd International Symposium on Polarization Phenomena of Nucleons, Karlsruhe, 1965*, edited by P. Huber and H. Schopper (Birkhäuser Verlag, Basel, 1966) p. 328.

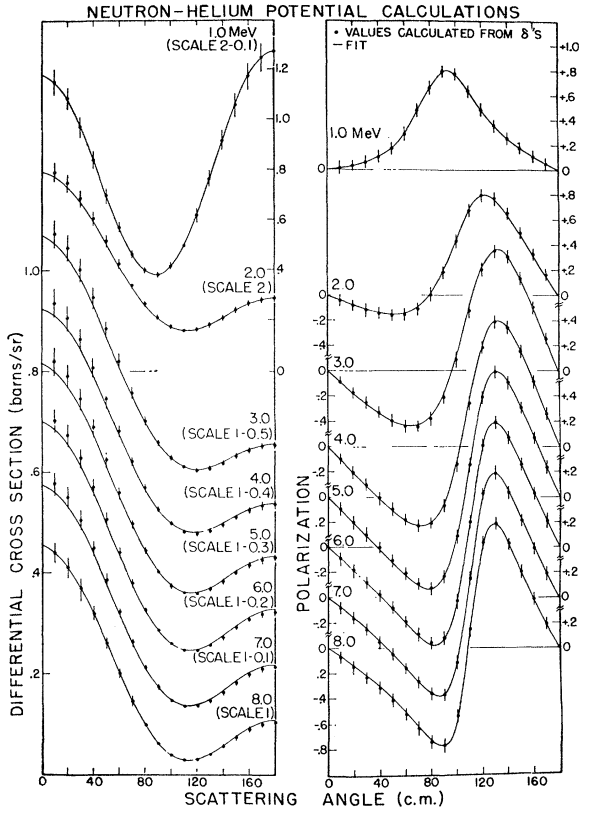

FIG. 19. Fits to neutron-helium scattering using a Saxon-Woods potential. The potential parameters used in these fits are given in Sec. IX.

around 90° and 60° from Ref. 20. Above 50 MeV, there are no phase-shift data with which to compare the single-level calculations. Actually, the phase shifts below 15 MeV are relatively insensitive to the choice of background parameters. The parameters which gave the best fit, i.e., the dashed curves in Fig. 18, when background resonances at 200 MeV with 60 MeV reduced widths were included, are

$$E_\lambda(P_{3/2}) = -4.24 \text{ MeV}, \quad \gamma_\lambda^2(P_{3/2}) = 10.94 \text{ MeV},$$
$$E_\lambda(P_{1/2}) = 2.61 \text{ MeV}, \quad \gamma_\lambda^2(P_{1/2}) = 15.06 \text{ MeV}.$$

IX. DISCUSSION OF THE SINGLE-LEVEL FITS

After utilizing single-level fits as a criterion for successfully determining the validity of a hard-sphere radius of 2.44 F for neutron-helium scattering below 7 MeV, it was found necessary to include a background resonance around 200 MeV in order to fit proton-helium and neutron-helium data at higher energies. The need for a higher-energy state could be real or it might be an indication of the inapplicability of the single level with the restrictions which have been imposed, such as requiring A to be independent of energy. Regardless of this complication, the single-level (with background) relation does yield satisfactory agreement to both proton- and neutron-helium scattering. The fact that the neutron-helium resonance parameters do not predict the same curve which the photon-helium phase shifts seem to fit best probably shows the inadequacy of the experimentally determined phase-shift sets to represent the scattering processes, rather than showing a difference in the resonance parameters (properly Coulomb corrected) in the He^5 and Li^5 systems. At this stage one should ignore the many reported phase-shift sets and make a χ^2 fit of all the polarization and cross-section data directly with curves computed from single-level phase shifts. This sizable task was not attempted but a different approach was tried, the preliminary results being given in the succeeding sections.

X. POTENTIAL-MODEL ANALYSIS

An attempt was made to find a Saxon-Woods potential which would represent the neutron-helium interaction. The results reported here are of a preliminary nature covering the energy range from 1 to 8 MeV. The full investigation, being carried out in collaboration with A. J. Elwyn, G. R. Satchler, and L. Owen, includes the energy range from 1 to 20 MeV for both the neutron-helium and proton-helium interactions.

So that there would be sensitivity to the spin-orbit parameters, polarization as well as cross-section values were *calculated* from the single-level phase shifts. Values were computed in 10° steps from 0° to 180° at neutron energies between 1 and 8 MeV. The phase shifts given in this paper were used for the calculations. A slightly modified version of the code[21] ABACUS-2 was used to adjust, for best fit, the parameters in a potential of the form

$$V(r) = -V_0 f(r) + V_{so}\left(\frac{\hbar}{mc}\right)^2 \frac{1}{r}\frac{d}{dr} g(r) \mathbf{l}\cdot\boldsymbol{\sigma},$$

where

$$f(r) = 1+\exp[(r-R)/a_0]^{-1},$$
$$g(r) = 1+\exp[(r-R_{so})/a_{so}]^{-1}.$$

Each energy was fitted individually, with all parameters adjusted for best fit. The resulting geometric parameters (R, a_0, R_{so} and a_{so}) were then averaged with respect to energy in order to obtain a set of parameters which were held constant over the entire energy range. A second search was then carried out in which V_0 and V_{so} were adjusted for best fit using the average geometric parameters.

The final fits are given by the curves in Fig. 19. The values used in the fitting procedure are represented by the points. The arbitrarily assigned uncertainties (for the fitting procedure) are represented by the error bars. In this search, an error of ± 0.05 was put on $P(\theta)$ and $\pm 0.05\,\sigma(\theta)$ on $\sigma(\theta)$. The quality of the fits is surprisingly

[21] E. A. Auerbach, Brookhaven National Laboratory Report No. BNL-6562, 1962 (unpublished).

good over the entire energy range, which includes the resonance near 1 MeV. (Direct comparison of the phase shifts is not as satisfying, possibly because this optical model predicted sizable d-wave phase shifts above 5 MeV, which is in disagreement with the analysis here and in earlier work. This difficulty will be covered in a later paper.) The parameters for these fits are

$$R=2.231\text{ F},\quad a_0=0.435\text{ F},$$
$$R_{so}=1.956\text{ F},\quad a_{so}=0.435\text{ F},$$
$$V_0=45.1-0.430\,E_n\text{ (MeV)},$$
$$V_{so}=3.95+0.144\,E_n\text{ (MeV)}.$$

The same geometric parameters were used in a search of V_0 and V_{so} for the proton-helium data from 2 to 5 MeV (higher energies are not considered here because at this time there is doubt as to the correct phase shifts in the energy region between 6 and 17 MeV). The input data consisted of the cross-section measurements of Barnard *et al.*[18] Again the polarizations were *calculated* from phase shifts. In this case, the set derived by Barnard *et al.* from his cross-section data was employed. The curves shown in Fig. 20 are the fits to the values represented by the points. The error bars on $\sigma(\theta)$ are those estimated by Barnard *et al.*, that is, $\pm 0.02\,\sigma(\theta)$. Errors of $\pm 0.05\,P(\theta)$ were assigned to the polarization values. The well-depth parameters are about the same as those for the neutron case.

A more ambitious program under way utilizes the raw data instead of fabricated data as above. Our hope is that this will be a suitable (if not the best) way to parametrize the neutron- and proton-helium scattering processes below 20 MeV. Other comments about the applicability of a Saxon-Woods–type optical model for the nucleon-helium interaction will be given in that report.

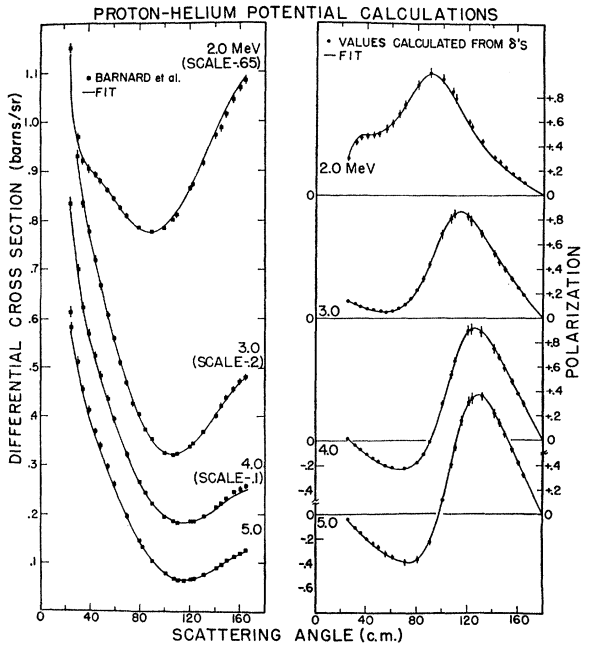

FIG. 20. Fits to proton-helium scattering using a Saxon-Woods potential. The geometric parameters used for these fits are the same as those used for the neutron-helium fits.

XI. SUMMARY AND DISCUSSION

Accurate angular distributions of neutron-helium scattering were obtained and are given for each energy in terms of three expansion coefficients. p-phase shifts derived under an assumption of hard-sphere s-wave scattering are in good agreement with the energy dependence predicted by a single-level (without background) resonance formula. The phase shifts also give polarization distributions which are in good agreement with the data of Sawers *et al.*[1] and of May *et al.*[6] at energies below 7 MeV. The present phase shifts are found to connect smoothly onto the phase shifts of HB[7] at energies above 8 MeV. A single-level resonance with a background level near 200 MeV gave a reasonable fit up to 18 MeV to the phase shifts obtained in this work and by HB. Since the p-wave phase shifts are quite dependent on the size of the s-wave phase shift in the present analysis and since there may be deviations at the higher energies from hard-sphere s-wave scattering, the phase shifts derived from the 5- to 7-MeV data are subject to some doubt. Therefore, the present authors place more confidence in the phase shift set based on the single level with background (columns 5, 6, and 7 in Table II). d-wave phase shifts for the energies above 6 MeV are not given here. The best reported set is probably that of HB.[7]

It is emphasized that the present cross-section *angular distributions* are of primary importance and should be considered independently from the phase shifts herein in future comparisons or analyses.

Phase shifts for proton-helium scattering also can be represented by a single-level (with background) resonance fit. In fact, the dashed curves shown in Fig. 18 probably are the best reported determination of these phase shifts in the region between 3 and 17 MeV. These phase shifts can be readily calculated from the resonance parameters given. (This method of "smoothing" the proton-helium phase shifts indicates the inconsistencies of the previously reported sets.)

An optical model employing a standard Saxon-Woods potential with reasonable parameters was found to represent neutron- and proton-helium scattering at the energies studied, i.e., below 8 and 5 MeV, respectively. A more thorough and ambitious optical-model analysis of all data up to 20 MeV is under way and is expected to give a better description of both neutron- and proton-helium scattering than the present resonance fits.

As for polarization experiments, the analyzing power of helium for neutrons is probably known now very well for energies up to 3 MeV. Above this energy, some

uncertainty still exists. A sensitivity study was made at numerous energies between 0.6 and 10.0 MeV in which all combinations of the phase shifts (given in columns 5, 6, and 7) $\pm 1°$ were used to calculate the polarization distribution. The same was done for $\delta \pm 2°$ above 10.0 MeV. Below 10 MeV it was found that the changes in the polarization at the angle near the positive maximum varied from the central value P_{pos} by about $\pm 0.03 P_{\text{pos}}$ The study with the larger increment showed variations around $\pm 0.07 P_{\text{pos}}$. If one considers the change in the average polarization for a 20° region centered near P_{pos} (a range typically used in polarization experiments) the effect is reduced by about 40%. Above 4 MeV there is also sizable (negative) polarization at forward angles. Since the cross section is relatively large here, this is the most efficient analyzing region. However, these sensitivity calculations show that the variations here are about 30% greater than those around P_{pos}. Thus, until more is known about the neutron-helium phase shifts, one is probably restricted to the region of the positive maximum for the more accurate investigations.

ACKNOWLEDGMENTS

The authors are indebted to M. M. Meier, R. S. Thomason, and Dr. L. A. Schaller for assistance in taking the data. We wish to thank Dr. F. O. Purser, Dr. W. Haeberli, Dr. G. R. Satchler, and Dr. R. B. Perkins for helpful discussions. Dr. N. R. Roberson and Dr. R. V. Poore are owed a debt of gratitude for their assistance with the on-line computer. Thanks are due to Dr. A. J. Elwyn for discussions and for allowing use of the potential-model calculations, which are in great part the product of his labor.

PHYSICAL REVIEW VOLUME 168, NUMBER 4 20 APRIL 1968

Proton-Proton Bremsstrahlung at 61.7 MeV*

M. L. HALBERT AND D. L. MASON†
Oak Ridge National Laboratory, Oak Ridge, Tennessee 37830

AND

L. C. NORTHCLIFFE‡
Texas A & M University, College Station, Texas 77843

(Received 6 November 1967)

The two final-state protons in the reaction $p+p \rightarrow p+p+\gamma$ at 61.7 ± 0.1 MeV were detected by $(\Delta E, E)$ telescopes placed at 30° on opposite sides of the beam. About 250 events were detected in a geometry with angular acceptance comparable to the maximum possible noncoplanarity. Additional data were obtained with apertures of smaller height, restricting the measurement to a more nearly coplanar geometry. The data indicate that the cross section is smaller for noncoplanar events. The estimated coplanar cross sections and differential cross section as a function of γ-ray angle are presented. The results agree with recent theoretical predictions.

I. INTRODUCTION

THE proton-proton bremsstrahlung (PPB) reaction, $p+p \rightarrow p+p+\gamma$, is of considerable current interest in the study of nuclear forces. The process involves different relative energies of the protons in the initial and final states and thus may provide information about matrix elements of the proton-proton interaction off the energy shell. Several years ago Sobel and Cromer[1] suggested that measurement of the PPB cross section might select among the different nucleon-nucleon potentials which describe elastic scattering equally well. The off-shell matrix elements enter into nuclear-matter calculations, and, indeed, may be important for any system having more than two nucleons.

The process was first studied experimentally at 158 MeV by Gottschalk, Shlaer, and Wang.[2–4] In their arrangement, often referred to as the Harvard geometry, the final-state protons were detected in coincidence by a pair of counter telescopes placed at equal angles on opposite sides of the beam. The total angle between the telescopes was less than that between scattered and recoil protons from p-p scattering so that elastic protons could not be detected in true coincidence. The energy of each proton was measured; with the known detector

* Research sponsored by the U. S. Atomic Energy Commission under contract with Union Carbide Corporation.

† Oak Ridge Graduate Fellow from the University of Florida under appointment from the Oak Ridge Associated Universities.

‡ Visiting scientist at Oak Ridge National Laboratory, 1965–66.

[1] M. I. Sobel and A. H. Cromer, Phys. Rev. **132**, 2698 (1963).

[2] B. Gottschalk, W. J. Shlaer, and K. H. Wang, Phys. Letters **16**, 294 (1965).

[3] B. Gottschalk, W. J. Shlaer, and K. H. Wang, Nucl. Phys. **75**, 549 (1965).

[4] B. Gottschalk, W. J. Shlaer, and K. H. Wang, Nucl. Phys. **A94**, 491 (1967).